processes

MDPI

Article

Effects of Methanol Application on Carbon Emissions and Pollutant Emissions Using a Passenger Vehicle

Zhao Zhang [1], Mingsheng Wen [1,*], Yanqing Cui [1], Zhenyang Ming [1], Tongjin Wang [1], Chuanqi Zhang [1], Jeffrey Dankwa Ampah [2], Chao Jin [2], Haozhong Huang [3] and Haifeng Liu [1,*]

1 State Key Laboratory of Engines, Tianjin University, Tianjin 300072, China; zh_zhao@tju.edu.cn (Z.Z.); yanqingcui@tju.edu.cn (Y.C.); 2019201306@tju.edu.cn (Z.M.); tongjin@tju.edu.cn (T.W.); zcq1224@163.com (C.Z.)
2 School of Environmental Science and Engineering, Tianjin University, Tianjin 300072, China; jeffampah@live.com (J.D.A.); jinchao@tju.edu.cn (C.J.)
3 College of Mechanical Engineering, Guangxi University, Nanning 530004, China; hhz421@gxu.edu.cn
* Correspondence: mingshengwen@tju.edu.cn (M.W.); haifengliu@tju.edu.cn (H.L.)

Abstract: Methanol, as a promising carbon-neutral fuel, has become a research hotspot worldwide. In this study, pure gasoline and gasoline blended with five different volume ratios of methanol (10%, 20%, 30%, 50%, and 75%) were selected as test fuels, which were referred to as M0, M10, M20, M30, M50, and M75. The experiments on carbon and pollutant emissions and performance were carried out on a passenger vehicle with gasoline direct injection (GDI) turbocharged engine using the steady-state, new European driving cycle (NEDC), and acceleration approaches. The results show that under steady-state conditions, as the methanol blending ratio increases, the volume of fuel consumption increases. Compared with pure gasoline, the equivalent fuel consumption and the CO_2 emissions are reduced by 0.95 L/100 km (10.6%) and 18.95 g/km (9.6%) in maximum extent by fueling M75, respectively. In the NEDC, the CO_2 emissions of M30 are reduced by 5.46 g/km (3.7%) compared with pure gasoline. After blending methanol in gasoline, CO emissions increase, and the emissions of NO_x, THC, and PM decrease. The acceleration time is shortened with the increase of blending ratio of methanol. The application of methanol reduces the combustion CO_2 emissions by 10% and improves the pollutant emissions.

Keywords: methanol; passenger vehicle; GDI engine; performance; emissions

Citation: Zhang, Z.; Wen, M.; Cui, Y.; Ming, Z.; Wang, T.; Zhang, C.; Ampah, J.D.; Jin, C.; Huang, H.; Liu, H. Effects of Methanol Application on Carbon Emissions and Pollutant Emissions Using a Passenger Vehicle. *Processes* **2022**, *10*, 525. https://doi.org/10.3390/pr10030525

Academic Editor: Zhihua Wang

Received: 22 January 2022
Accepted: 4 March 2022
Published: 7 March 2022

1. Introduction

Having undergone development of more than 100 years, internal combustion (IC) engines have become a remarkable part of the world manufacturing economy [1–3] and are widely used in ship transportation, construction machinery, aerospace, private vehicles, and other transport fields [4–8]. Although traditional fuel vehicles have been influenced by new energy vehicles in recent years [9–12], most of the world driving force could still be dominated by IC engines until 2040 [13]. Therefore, the IC engines still have sufficient development potential [14–16]. To address the issue of global warming, global efforts are underway to achieve net zero emissions by 2050 [17,18]. The promotion and application of carbon-neutral fuels is a notable way to achieve net zero emissions for IC engines [19,20]. Hence, the research of relevant carbon-neutral fuels has become a hotspot in the field of IC engines [21,22]. On the other hand, in the transportation sector, gasoline is a prominent energy source, and the vehicles of 89% in China are fueled with gasoline [23]. Consequently, researchers from various countries have made efforts to investigate the suitable alternative fuels for gasoline (for instance, carbon-neutral alcohol fuels) while developing increasingly advanced engine technologies in recent years [24–28].

Decades of research on alternative fuels showed that alcohol fuel is one of the most appropriate fuels for gasoline [29–32]. Methanol, as carbon-neutral fuel, is a colorless,

transparent, volatile, flammable, and renewable liquid [33–37], and has higher octane number and oxygen content, faster flame propagation speed, and no C-C bond [38]. These properties of methanol could reduce the local fuel-lean and fuel-rich zones in the cylinder to decrease fuel consumption and emissions caused by frequent acceleration and deceleration. Since the composition of the combustion products and flame propagation speed are significantly different for local fuel-lean and fuel-rich zones [39–41]. Moreover, the industrial technology for preparing methanol is very mature, which has low production cost [42], and technology equipment is relatively complete and easy to popularize [43]. Therefore, methanol, as one of the most promising carbon-neutral fuels, has become a research hotspot for alternative fuels of IC engines in recent years [44–46].

Methanol can be synthesized from renewable biomass, and converted from fossil fuels or produced by hydrogenation with carbon dioxide (CO_2) [47,48], which is a potential development method for industrial methanol production [49]. The conversion of CO_2 to methanol can also alleviate the global warming situation. Lian et al. [50] used Fe-Cu/γ-Al_2O_3 as a catalyst to produce methanol from CO_2 in a heat-insulated warm plasma-catalytic reactor and found that the conversion rate of CO_2 to methanol was as high as 94%. Bansode and Urakawa [51] used Cu/ZnO/Al_2O_3 as catalyst, and it was found that the conversion rate of CO_2 to methanol was greater than 95%. On the other hand, worldwide researchers have studied the characteristics of combustion and emissions of methanol-gasoline blends on engines. The effects of methanol-gasoline blends on port fuel injection (PFI) engine were investigated by Liu et al. [52]. The results manifested that after three-way catalytic converter, the conversion efficiency of nitrogen oxide (NO_x), carbon monoxide (CO), and hydrocarbon (HC) was very high, but unburned methanol and formaldehyde increased as the volume ratio of methanol increased. Nuthan et al. [53] investigated the combustion and emissions characteristics of an equal volume ratio of methanol-gasoline blended fuel (M50) and pure gasoline in a gasoline engine. Results suggested that the emissions of HC, CO, and NO_x of M50 decreased between 30% and 40% by comparison with pure gasoline. Meanwhile, compared with pure gasoline, the brake thermal efficiency of M50 was increased by 25%. The effects of methanol-gasoline fuel on modified homogeneous charge compression ignition (HCCI) engine were investigated by Maurya and Agarwal [54]. The research results demonstrated that compared with pure gasoline, methanol had lower ignition point, and the combustion efficiency of methanol was higher (99%) under the conditions of higher intake air temperatures and fairly rich mixture, while the combustion efficiency of gasoline was only 96%. Therefore, methanol was a good substitute for gasoline in HCCI engines.

Some studies focused on the unregulated emissions of the engines using methanol as alternative fuel. Hua et al. [55] measured the content of polycyclic aromatic hydrocarbons (PAHs) using the methanol-gasoline mixture at four methanol volume fractions, which were 20%, 40%, 60%, and 80% (M20, M40, M60, and M80), on the burner. The results demonstrated that the addition of methanol significantly inhibited the production of PAHs. Wei et al. [56] used methanol-gasoline mixture with methanol volume fractions of 10%, 20% and 85% (M10, M20 and M85) on a spark ignition engine to explore the content of unburned formaldehyde and methanol in the emissions. The experiment results declared that compared with neat gasoline, the formaldehyde emissions were doubled in M10 but decreased significantly in M20 and M85. Zhang et al. [57] measured the content of unburned methanol emissions in a PFI gasoline engine with pure gasoline and M10, M15, M20, and M30. Results revealed that with the increase of methanol blending ratios, the content of unburned methanol emissions increased almost linearly. Furthermore, there are others studies focused on vehicles using methanol. The impacts of the amount of methanol injection per cycle and ambient temperature on the vehicle cold start were studied by Li et al. [58]. Results suggested that when the ambient temperature was below 16 °C, injecting a large amount of methanol per cycle started the engine unsteadily. However, the unburned HC emissions of methanol-gasoline blends reduced significantly during the vehicle cold-start when the ambient temperature increased. Wang et al. [59] researched

the effects of methanol-gasoline blend on gasoline direct injection (GDI) passenger vehicle during the new European driving cycle (NEDC) and compared the results to conventional gasoline. The experimental results implied that methanol-gasoline blends significantly decreased pipe-out HC and CO emissions. The use of methanol-gasoline blends generated about 0.8–4.1% less pipe-out CO_2 emissions than baseline gasoline while saving fuel cost by 5.7–15%.

Based on the above literature reviews, it can be concluded that many studies focused on the combustion and emissions characteristics of methanol-gasoline blends at low and medium blending ratios. Similar studies considering a relatively higher volume ratio of methanol are limited, especially in the passenger vehicle. However, the blending ratio of methanol in gasoline is higher, the requirement for fossil fuels will be reduced, and CO_2 emissions of fossil fuels will also be reduced. Therefore, researching the effects of blending high ratio methanol in gasoline is conducive to filling in the research gap. Furthermore, the technologies of gasoline engine have undergone tremendous changes with the continuous development of technology, and it is necessary to conduct more in-depth and comprehensive research on the application of methanol in modern gasoline engines. In the current study, different ratios of methanol-gasoline blends, including low, medium, and high blends were employed to test on a passenger vehicle with GDI turbocharged engine. The aim of the study presented here was to investigate the effects of different blending ratios of methanol in gasoline-methanol blends on the characteristics of fuel consumption, emissions and acceleration of vehicle, providing a reference for the application of methanol on passenger vehicles.

2. Experimental Setup and Methodology

2.1. Experimental Facilities

The experiments were conducted on the passenger vehicle with GDI engine produced and sold in China, and the main parameters of the GDI engine are shown in Table 1. Figure 1 is a schematic diagram of the chassis dynamometer test bench, which can simulate the actual road driving during experiments. The exhaust gas was introduced into the air through the dilution channel. The dilution channel simulated the process of the exhaust gas entering the atmospheric environment. At the same time, a segment of exhaust was introduced and stored in the airbag. Throughout the test process, the emission analyzer continuously measured the gaseous emissions of the diluted exhaust. At the end of the experiment, the diluted exhaust components stored in the airbag were analyzed. The results of fuel consumption and gaseous emissions came from the analysis of the airbag components and the results of particulate matter (PM) emissions were derived from precision electronic balance. Table 2 is the specifications of the main experiment equipment used in this research, and Table 3 shows the measurement error range of experimental equipment.

Table 1. Main parameters of the GDI engine.

Project	Parameters
Cylinder number	4
Displacement (L)	1.4
Cylinder bore (mm)	74.5
Compression ratio	10.5
Intake system	Turbocharged
Maximum power	96 kW/5000–6000 rpm
Injection system	GDI

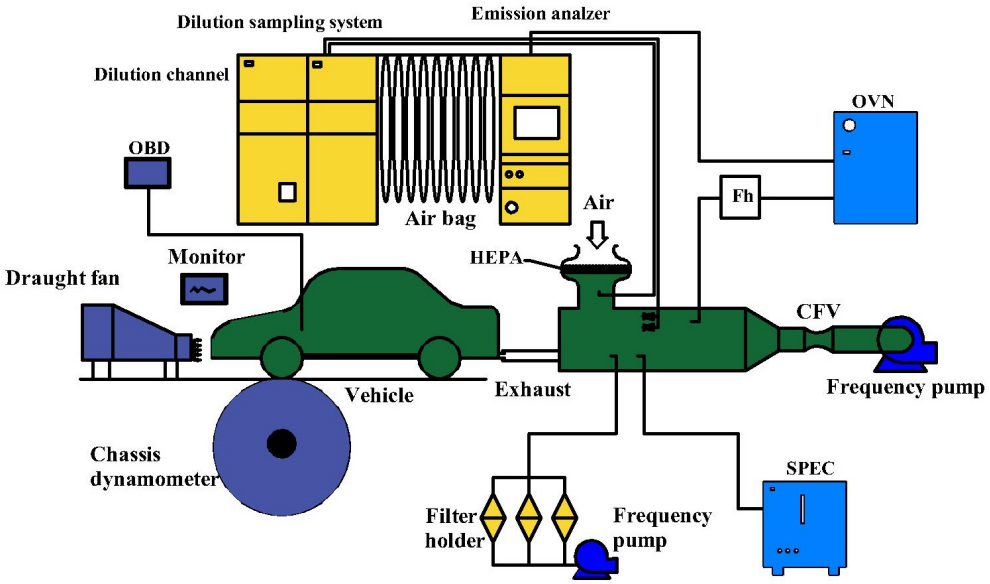

Figure 1. The schematic diagram of the chassis dynamometer. CFV = critical flow venturi; HEPA = high efficiency particulate air filter; OVN = oven type heated analyzer.

Table 2. Main test equipment.

Parameter	Model Specifications	Manufacturer
Chassis dynamometer	Roadsim48″compact	Austria AVL
Filter paper	EMFAB-TX40H120-WW	American PALL
Solid particle counting system	MEXA-2000SPCS	Japan Horiba
Precision electronic balance	MSE6.6S-000-DF	German Sartorius
Emission analyzer	MEXA-7200H	Japan Horiba
Dilution channel	DLS-7100E	Japan Horiba
Dilute sampling system	CVS-7200T	Japan Horiba
On board diagnostics	X431	China LAUNCH

Table 3. Uncertainties of measured parameters [60].

Equipment	Test Project	Measurement Errors
Chassis dynamometer	Constant traction tolerance	<0.2% full scale
	Constant speed difference	<0.05% full scale
	Time measurement tolerance	0.00005%
Emission analyzer	CO_2	≤1% of full scale or 2% of measured value, whichever is the smallest
	NOx	
	CO	
	THC	
Precision electronic balance	Filter paper quality	±1 μg

2.2. Experimental Methodology

The steady-state experiment was set at different stable speeds (15, 65, and 120 km/h) to study the effects of different methanol blending ratios on performance and emissions of GDI vehicles. The tests were carried out under hot engine conditions, since once the methanol blending ratios were more than 30%, the vehicle cannot be cold started. To guarantee the reliability of experimental data, before the measurement, the vehicle accelerated from 0 km/h, vehicle speed during gear shifting and acceleration refer to NEDC, and operated firmly at 15, 65, and 120 km/h, respectively. The vehicle operated steadily in 20 s during the experiment. The tested fuel and additives are limited, and the test data were recorded only once.

The NEDC was employed to test fuel consumption and emissions of the vehicle. The whole cycle of NEDC was divided into extra urban driving cycle (EUDC) and urban driving cycle (UDC). Compared with EUDC, the UDC operating speed is lower, which has cold start process with lower engine temperature. Figure 2 shows the specific speed of UDC, EUDC, and NEDC. The NEDC tests were conducted by experienced drivers. It ensures that the error between the actual speed and the theoretical speed is within 1 km/h, which was basically consistent with the theoretical speed of NEDC.

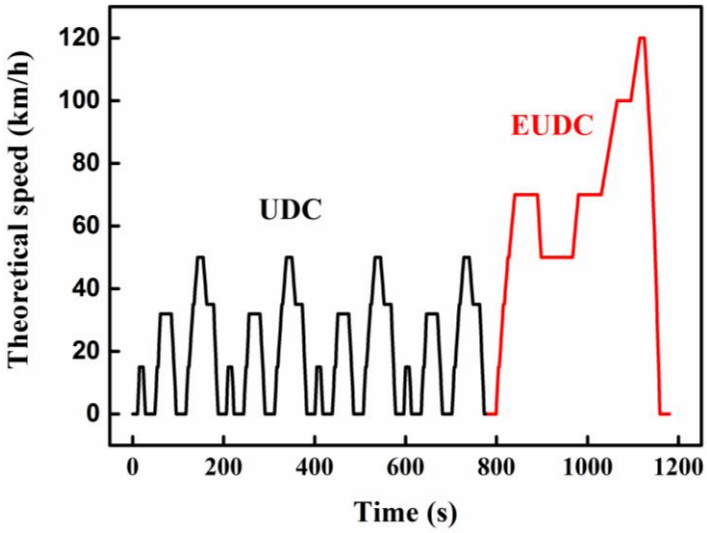

Figure 2. The theoretical speed speeds of NEDC [60].

The acceleration experiment was conducted to compare the effects of methanol-gasoline blends on acceleration performance of the vehicle. Since the passenger vehicle has a manual transmission, to eliminate the error caused by the gear shift process, each gear was measured separately, referring to the minimum and maximum speeds of the stable operation of vehicle. Finally, the third, fourth, and fifth gear speeds were 30~65, 40~80, and 60~110 km/h, respectively. The time required from the lowest speed to the highest speed was used to estimate the acceleration performance.

To reduce the influence of other factors, the tires were checked before the experiment, and the pressure was always maintained at 0.22~0.23 MPa. The electronic control unit (ECU) was not calibrated, and the engine used the original MAP. If the engine did not knock, spark timing was automatically advanced in the ECU. Similar trends have been found in previous studies of other alternative fuels [60,61]. When changing the test fuel, the vehicle ran at idle speed to completely empty the previous fuel in the fuel tank, the fuel pipe and the fuel filter were replaced. After changing the test fuel, to eliminate the interference of previous test fuels, the vehicle ran at a speed of about 60 km/h for more than 15 min. It is worth noting that in order to focus on the effects of fuel properties on the combustion and raw emissions characteristics, the three-way catalyst converter was disabled before the test. Since during the test, the properties of fuels are quite different, and the three-way catalyst converter may be aged and invalid, which makes the test results inaccurate. Certainly, in addition to removing the three-way catalyst converter, the rest of the whole vehicle is the test object, and the knock sensors are installed and always work.

2.3. Experimental Fuels

The gasoline and methanol used in this study were provided by China Petroleum and Chemical Corporation, and the specific properties, as seen from Table 4, were measured by the experiment. Methanol has higher oxygen content, which can achieve approximately 50%, and higher octane number in contrast with neat gasoline. The latent heat of vaporization for methanol is also relatively higher, but the low heating value is lower than that

of gasoline. In this study, five different volume proportions of methanol (10%, 20%, 30%, 50%, and 75%) were added to gasoline, which were referred to as M10, M20, M30, M50, and M75, and the pure gasoline was the baseline fuel (M0).

Table 4. Main properties of methanol and gasoline.

Parameters \ Fuels	Methanol	Gasoline
Molecular formula	CH_3OH	C_4–C_{12}
Octane number	111	92
Density (kg/L) @ 30 °C [62]	0.796	0.745
Latent heat of vaporization (kJ/kg)	1170	180–373
Boiling point (°C)	65	35–215
Lower heating value (MJ/L)	19.93	43.40

3. Results and Discussion

3.1. Effects of Blending Ratios of Methanol on Fuel Consumption and Emissions of Vehicle at Different Steady Speeds

Figure 3a,b show the effects of different methanol blending ratios on the fuel consumption and equivalent fuel consumption at different steady speeds, respectively, with the relative values of fuel consumption and equivalent fuel consumption labeled above the bars. As shown in Figure 3a, the volumetric fuel consumption gradually increases with the increase of methanol blending ratio. The maximum relative difference is obtained by fueling M0 and M75 at medium speed, with a value of 54.4% (2.34 L/100 km). The root cause behind these results is that the lower heating value of methanol is much lower than that of pure gasoline, approximately half that of gasoline. Briefly, the volumetric fuel consumption has a strong negative correlation with lower heating value. Hence, the volumetric fuel consumption of the vehicle fueled with the methanol-gasoline blends increase at the same heat release of the pure gasoline vehicle. Furthermore, the overall fuel consumption is the lowest at the speed of 65 km/h, followed by 120 km/h, which may be related to the better fuel economy of the vehicle at medium and high speeds. It can also be seen from Figure 3a that the discrepancies of M50 and M75 are minor at the speed of 15 km/h, which may be attributed to the unstable combustion at lower engine speeds and higher blending ratio of methanol. Figure 3b is the equivalent fuel consumption obtained after converting the lower heating value of various test fuels into that of pure gasoline (M0), which can reflect thermal efficiency to a certain extent. It highlights that the equivalent fuel consumption reduces when the engine is fueled with methanol-gasoline blends at medium and high speeds. But the irregular influence of methanol-gasoline blends on the equivalent fuel consumption at low speed. At medium and high speeds, this could be attributed to the higher-octane number of methanol, the spark timing advances automatically in the ECU when the engine is fueled with methanol-gasoline mixtures. The advanced spark timing increases the combustion constant volume degree, improving the thermal efficiency and reducing the equivalent fuel consumption. On the other hand, the flame propagation speed of methanol is faster, which shortens combustion duration, improving the combustion constant volume degree and the thermal efficiency of the engine. However, at low speed, the higher latent heat of vaporization for methanol causes a decrease of in-cylinder temperature. In order to ensure higher exhaust temperature and aftertreatment efficiency, the original ECU delays the ignition timing, resulting in the reduction of combustion constant volume degree [60]. However, the retarded ignition timing that can be realized is limited, and the equivalent fuel consumption of M75 is basically the same as that of M50. Meanwhile, both M75 and M50 are close to the limit of spark ignition timing, but M75 has higher oxygen content and faster combustion flame propagation speed, which improves the combustion duration and reduces the equivalent fuel consumption. The equivalent fuel consumption of M75 is reduced by 0.95 L/100 km (10.6%) at the speed of 15 km/h compared with M0.

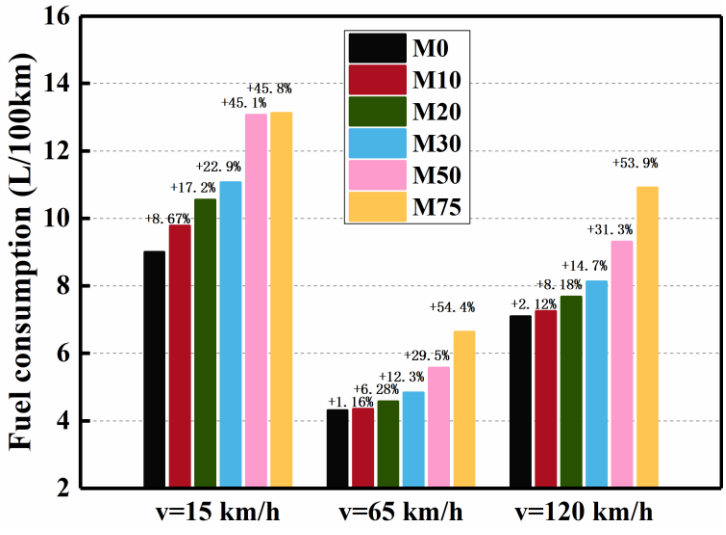

(**a**) The volumetric fuel consumption

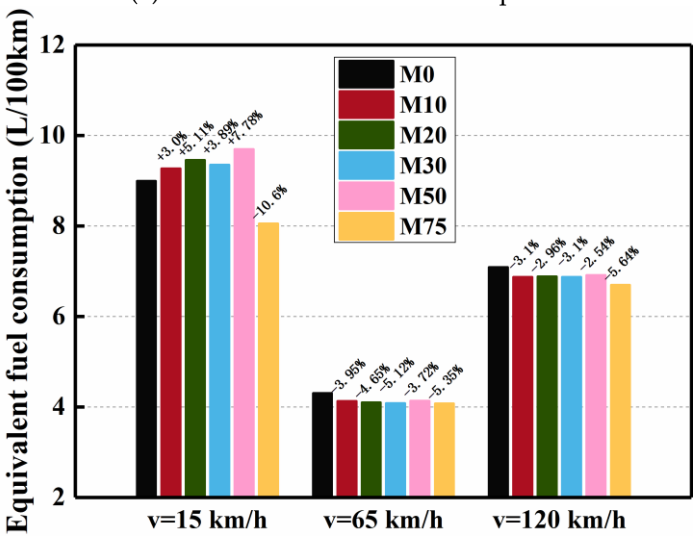

(**b**) The equivalent fuel consumption

Figure 3. Effects of different methanol blending ratios on fuel consumption at different vehicle speeds.

Figure 4 denotes that it is beneficial for blending methanol in gasoline to reduce CO_2 emissions at medium and high vehicle speeds. But the blends are detrimental at low speed, except for a larger proportion of methanol. It should be noted that the trends of CO_2 emissions are similar to those of the equivalent fuel consumption, and the main reason is that the CO_2 emissions are attributed to the equivalent fuel consumption and H-C ratio of fuels. The H-C ratio of methanol is relatively higher, and the CO_2 emissions decrease as the methanol increases. Further, the equivalent fuel consumption is reduced as methanol is added into the gasoline at medium and high vehicle speeds. Therefore, CO_2 emissions are lower as using the blending fuel of methanol and gasoline. But the equivalent fuel consumption is higher as using methanol-gasoline at low speed due to the discussions mentioned above. Meanwhile, the lower H-C ratio can not offset the loss of equivalent fuel consumption, so CO_2 emissions increase at low speed. The CO_2 emissions of M75 are reduced by 18.95 g/km (9.6%) at the speed of 15 km/h compared with M0.

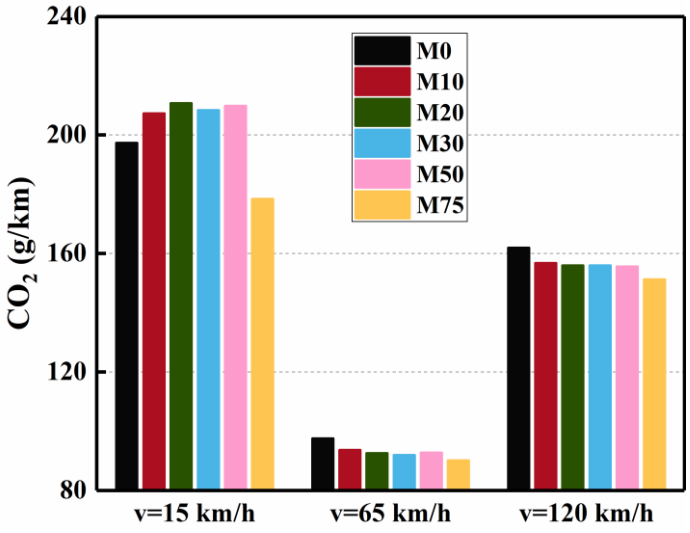

Figure 4. Effects of different methanol blending ratios on CO_2 emissions at different vehicle speeds.

Figure 5 demonstrates the effects of different methanol blending ratios on NO_x emissions. An interruption form is employed to consider the NO_x emissions are relatively higher at the speed of 120 km/h. Overall, gasoline blended with methanol reduces NO_x emissions, and the reduction degree is highest at the speed of 15 km/h. The oxygen content of methanol is higher, reaching 50%. Therefore, as the blending ratio increases, the oxygen content of methanol-gasoline blend increases, which is beneficial to promote the NO_x generation. However, the latent heat of vaporization for methanol is relatively higher, as seen from Table 4, causing the in-cylinder temperature of engine to decrease, which inhibits the NO_x formation. The preceding two conditions influence the NO_x emissions of vehicles at the same time, the reduced in-cylinder temperature is the dominant factor, causing NO_x emissions to decrease after gasoline mixed with methanol. Meanwhile, it is also observed that the overall NO_x emissions are relatively higher at the speed of 120 km/h, which is attributed to the higher in-cylinder temperature. The maximum relative difference of NO_x emissions is obtained by fueling M0 and M75 at 15 km/h, respectively, which differs by 79.1% (345.54 mg/km).

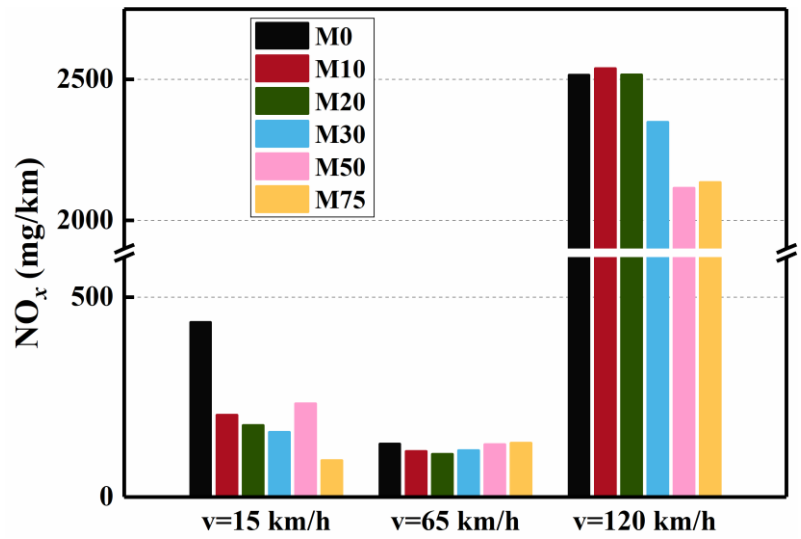

Figure 5. Effects of different methanol blending ratios on NO_x emissions at different vehicle speeds.

Figure 6 shows the effects of different methanol blending ratios on CO emissions at different vehicle speeds, which demonstrates that CO emissions decrease after gasoline

blended with methanol in most cases. Compared with M0, the CO emissions of M75 are reduced by 4491.4 mg/km (70.2%) at the speed of 15 km/h. CO is a product of incomplete combustion. On one hand, the higher oxygen content of methanol promotes combustion completely, which profits the oxidation of CO. On the other hand, the higher latent heat of vaporization for methanol causes a decrease of in-cylinder temperature, which may wreck the oxidation path of CO to CO_2, increasing CO generation. The simultaneous effects of these two aspects lead to that the overall trend of CO emissions decrease as methanol blending ratios increase. The retarded spark timing for M50 and M75 results in lower in-cylinder temperature at low speed, which increases CO emissions of M50 and M75. But M75 has higher oxygen content, which improves CO emissions. CO emissions of M20 are inflection points at low and high speeds, and their values decrease less, which are basically similar to those of gasoline. At low speed, the reason may also be the lower in-cylinder temperature and insufficient oxygen, resulting in the least reduction of CO emissions. At high speed, the less mixing and combustion time makes the above problems more prominent, so the CO emissions of M20 are slightly higher than those of gasoline. It should be noted that CO emissions are relatively higher at the low speed, while the results are the opposite at the medium and high speed, which may be related to the higher in-cylinder temperature at higher speeds. A higher in-cylinder temperature facilitates the conversion of CO to CO_2, reducing CO emissions. But the combustion duration is shortened significantly at high speed. CO has not enough time to completely oxidize, which leads to the increased CO emissions at 120 km/h compared with those of 65 km/h.

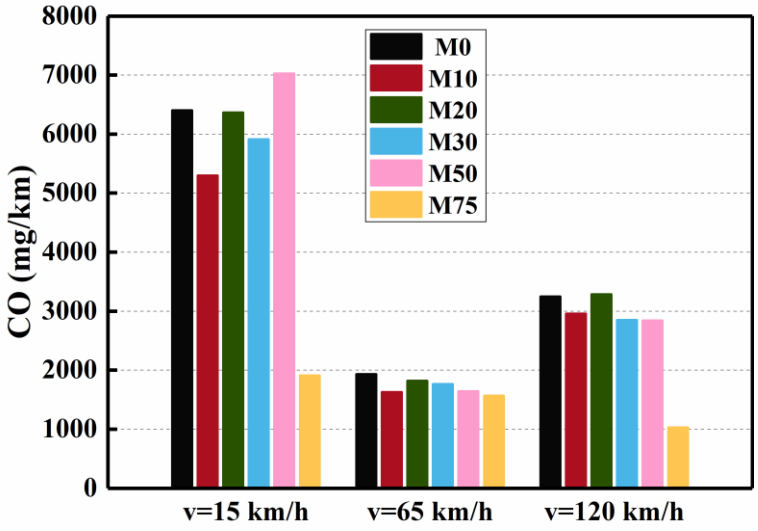

Figure 6. Effects of different methanol blending ratios on CO emissions at different vehicle speeds.

The effects of different methanol blending ratios on total hydrocarbon (THC) emissions at different vehicle speeds are shown in Figure 7, which manifests the THC emissions decrease asymptotically with the increase of methanol blending ratios except for the vehicle speed of 15 km/h. It should be noted that the maximum relative difference of THC emissions is obtained by fueling M0 and M30 at 15 km/h, respectively, which differs by 59.9% (1225.48 mg/km). The higher-octane number of methanol prolongs ignition delay, which is conducive to forming uniform fuel-air mixture, reducing in-cylinder fuel-rich zones and the HC generation. On the other hand, the higher oxygen content of methanol promotes complete combustion, which in turn reduces THC emissions. The overall THC emissions at low speed are higher than those at medium and high speeds, and the reasons are similar to the discussions of CO emissions. It is also due to the fac that the lower in-cylinder temperature at low speed inhibits the conversion of HC to CO_2, increasing THC emissions. Moreover, lower in-cylinder temperature results in higher THC emissions of

M50 and M75 due to retarded ignition timing. However, M75 has a higher oxygen content, which improves THC emissions at low speeds.

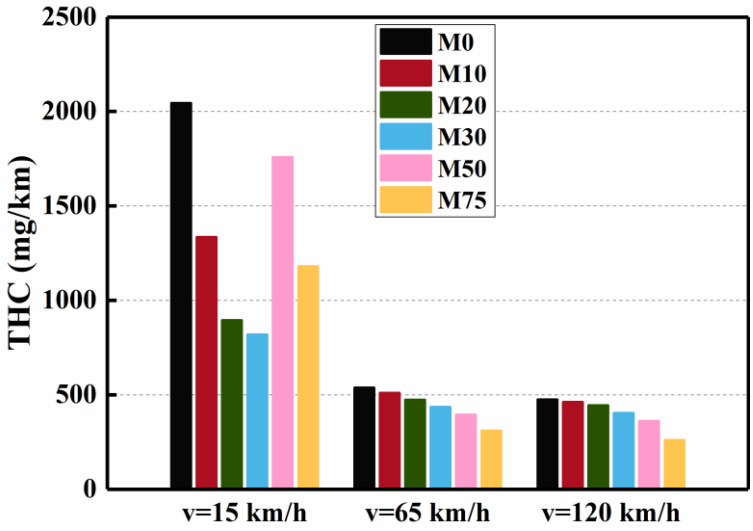

Figure 7. Effects of different methanol blending ratios on THC emissions at different vehicle speeds.

3.2. Effects of Small Proportions of Methanol on Fuel Consumption and Emissions under NEDC

Since the requirement of cold start under NEDC, a large proportion of methanol blending results in lower in-cylinder temperature, extremely unstable combustion, and even misfire. Therefore, only the impacts of lower blending ratio of methanol on vehicle performance and emissions are presented in this section. Figure 8a,b show the effects of different methanol blending ratios on volume fuel consumption and equivalent fuel consumption under NEDC, respectively, and the values of fuel consumption are labeled above the bars. The results highlight that the volume fuel consumption asymptotically increases as the methanol blending ratio increases, as shown in Figure 8a. The reasons correspond with the discussions of steady-state conditions. As mentioned earlier, the root cause behind the results is that the volume fuel consumption has a strong negative correlation with lower heating value. Therefore, the volume fuel consumption of the vehicle fueled with the methanol-gasoline blends increase at the same heat release as that of pure gasoline vehicle. It is interesting to note that the overall volume fuel consumption under UDC is higher than that under EUDC. The main reason is that the vehicle frequently accelerates and decelerates during UDC, resulting in fuel-lean and fuel-rich zones in the cylinder of engine, which in turn leads to incomplete combustion and increases fuel consumption. It is worth noting that the difference between the minimum and maximum fuel consumption is obtained by fueling M30 and M0 in the NEDC, respectively, which differs by 1.06 L/100 km (16.2%). It depicts that the equivalent fuel consumption reduces during the NEDC when the engine is fueled with methanol-gasoline blends, seen from Figure 8b. The reasons correspond with the discussions of steady-state conditions. As mentioned earlier, the higher-octane number and the faster flame propagation speed of methanol improve the thermal efficiency of the engine. Higher equivalent fuel consumption of methanol-gasoline blends comes from the UDC with more low speed. The reason also is that retarded ignition timing causes the reduction of combustion constant volume degree. The difference between the minimum and maximum equivalent fuel consumption is obtained by fueling M30 and M0 in the NEDC, respectively, which differs by 0.11 L/100 km (1.67%).

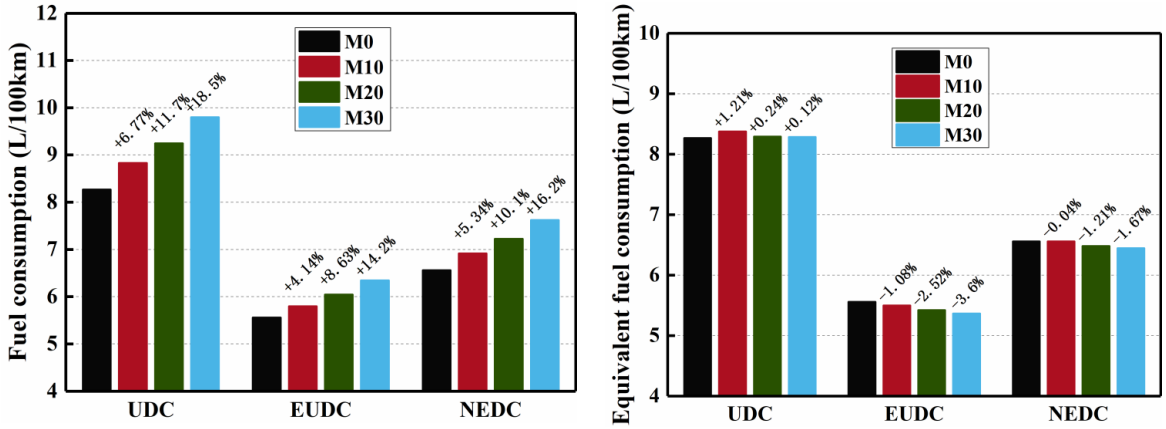

(**a**) The volume fuel consumption (**b**) The equivalent fuel consumption

Figure 8. Effects of different methanol blending ratios on fuel consumption under NEDC.

The effects of different methanol blending ratios on gaseous emissions are shown in Figure 9. Figure 9a reveals that blending methanol in gasoline generally favors reducing CO_2 emissions in the NEDC. The mechanism of decreased CO_2 emissions is mentioned in the above section of stable speed. The CO_2 emissions are attributed to the equivalent fuel consumption and H-C ratio of fuels. Although the equivalent fuel consumption of methanol-gasoline blends is higher than that of gasoline under UDC, but the H-C ratio of M20 and M30 with higher methanol blending ratio is improved more obviously. Therefore, the CO_2 emissions of M20 and M30 are lower than those of gasoline under UDC. Since the equivalent fuel consumption of M10 is slightly higher than that of gasoline in UDC and is slightly lower than that of gasoline in EUDC, and the improvement of H-C ratio is limited, which can not offset the increase of CO_2 emissions. CO_2 emissions of M10 are higher in UDC and lower in EUDC than that of gasoline. Finally, the CO_2 emissions of M10 are basically the same as those of gasoline in NEDC. The difference between the maximum and minimum CO_2 emissions is obtained by fueling M0 and M30 in the NEDC, respectively, which differs by 5.46 g/km (3.7%). As the methanol blending ratio increases, NO_x emissions gradually decrease, as shown in Figure 9b. As mentioned earlier, the higher latent heat of vaporization of methanol promotes the reduction of the in-cylinder temperature, which affects the NO_x formation adversely. However, the higher oxygen content of methanol supports the NO_x formation. The interaction between preceding two factors causes the decrease of NO_x emissions with the increase of methanol blending ratio. It is worth noting that the NO_x emissions under UDC are lower than those under EUDC, which is related to the higher in-cylinder temperature in the EUDC. The difference between the minimum and maximum NO_x emissions is obtained by fueling M30 and M0 in the NEDC, respectively, which differs by 194.66 mg/km (19.3%). Figure 9c demonstrates that CO emissions decrease first and then increase with the increase of methanol in the NEDC. Compared with M0, the CO emissions of M30 are increased by 1052.54 mg/km (24.1%) in the NEDC. CO emissions mainly come from the UDC with more low speed. Since CO emissions are strongly related to combustion temperature [63]. M10 with lower methanol blending ratios has less effects on combustion temperature, and its proper oxygen content improves the CO oxidation. However, M20 and M30 of higher latent heat of vaporization and retarded combustion phasing significantly reduce the combustion temperature, which dominates the increase of CO emissions. THC emissions increase first and then decrease with the increase of methanol in the NEDC, as shown in Figure 9d. Compared with M0, the THC emissions of M30 are decreased by 111.31 mg/km (10.9%) in the NEDC. Compared with CO, HC can be oxidized at lower combustion temperature, so the THC emissions are significantly lower than CO emissions. Although higher methanol blending ratio leads to lower combustion temperature, there is no strong correlation between THC emissions and combustion temperature [63]. So, the methanol-gasoline blends of higher methanol

blending ratio and oxygen content can also promote HC oxidation at lower temperature. It should be noted that the emissions of CO and THC under UDC exceed those under EUDC. First of all, the vehicle frequently accelerates and decelerates under UDC, which leads to the formation of fuel-lean and fuel-rich zones in the cylinder, increasing the emissions of CO and THC. Secondly, the higher vehicle speed under EUDC results in the higher in-cylinder temperature, which is conducive to complete combustion and decreasing the emissions of THC and CO. Finally, during cold engine starting, fuel-rich injection is required to ensure ignition in the first 30 s, and excessive fuel supply due to poor mixing in the cylinder and low temperature produces large amounts of CO and THC emissions during cold starts.

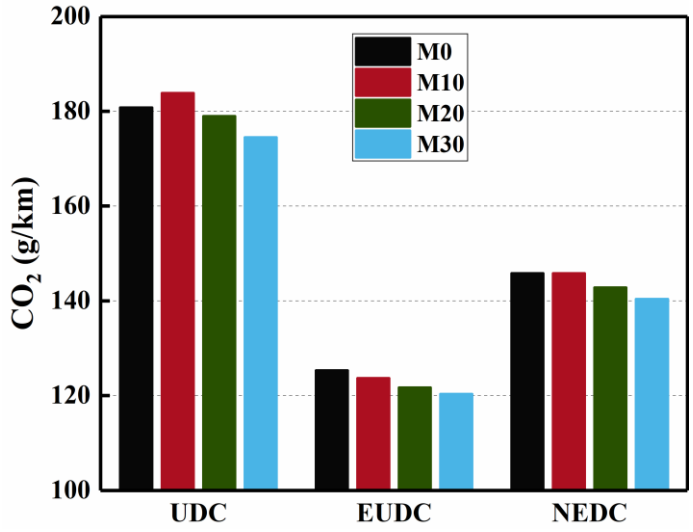

(**a**) CO_2 emissions

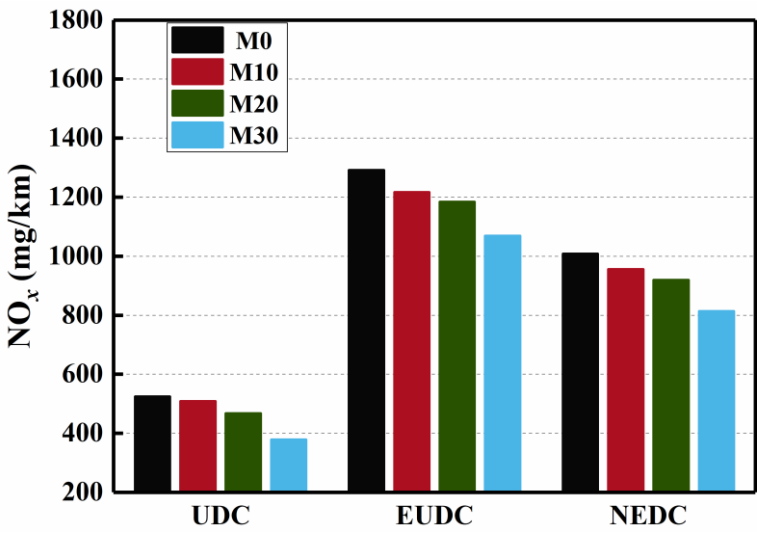

(**b**) NO_x emissions

Figure 9. *Cont.*

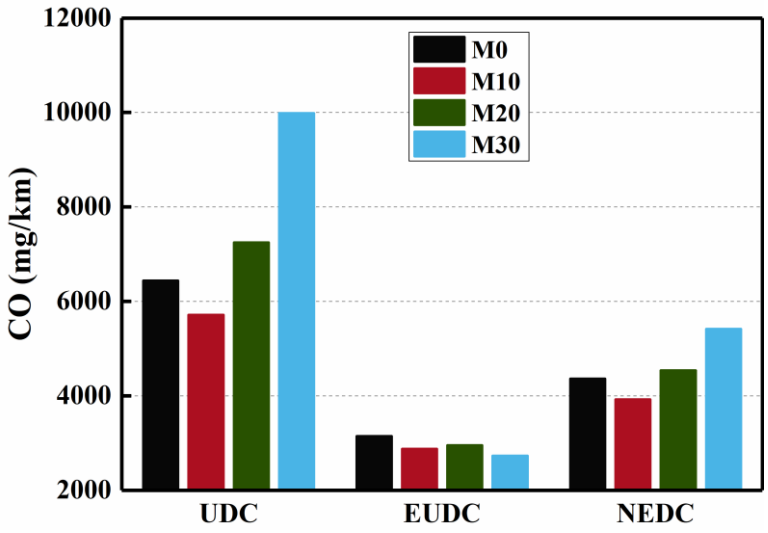

(**c**) CO emissions

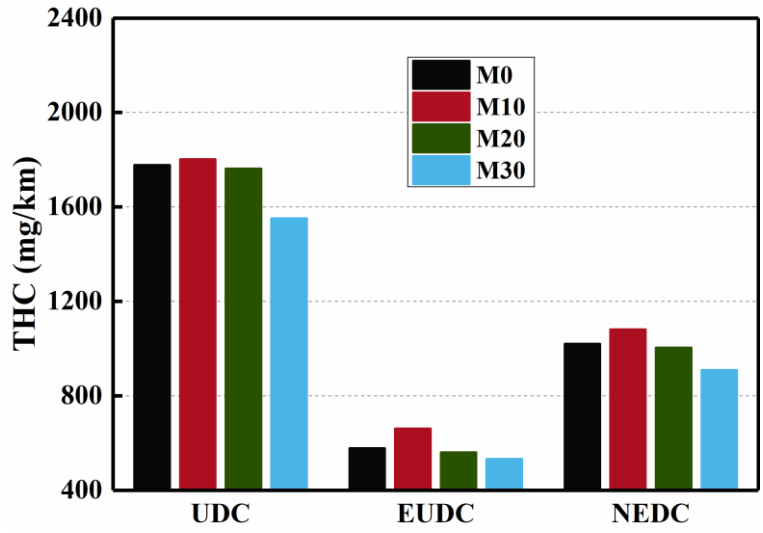

(**d**) THC emissions

Figure 9. Effects of different methanol blending ratios on gaseous emissions under NEDC.

The effects of different test fuels on PM emissions are shown in Figure 10, which suggests that the PM emissions of M10, M20, and M30 are lower than those of M0. On the one hand, the higher oxygen content of methanol is conducive to reducing the production of PM consequently. On the other hand, the higher latent heat of vaporization of methanol decreases the in-cylinder temperature and suppresses the oxidation of PM emissions. At lower methanol blending ratio, the main reason for the increased PM emissions is the lower oxygen content of the fuel. At higher methanol blending ratio, the main reason for the increased PM emissions is the higher latent heat of vaporization of the fuel. The PM emissions under EUDC exceed those under UDC. Since more fuel mass is injected at high speed, the mixing time is shortened, and the PM emissions increase accordingly. M30 under EUDC has longer injection duration, more spray impingement and more PM generation near the wall. The above factors interact with each other, resulting in the results of Figure 10. It should be noted that the improvement degree of PM emissions is greater during the UDC when the vehicle is fueled with methanol-gasoline blends. The possible reason is that the higher oxygen content of methanol reduces the local fuel-lean and fuel-rich zones in the cylinder caused by frequent acceleration and deceleration. It is worth noting that the difference between the minimum and maximum PM emissions is obtained by fueling M20 and M0 in the NEDC, respectively, which differs by 8.32 mg/km (47.9%).

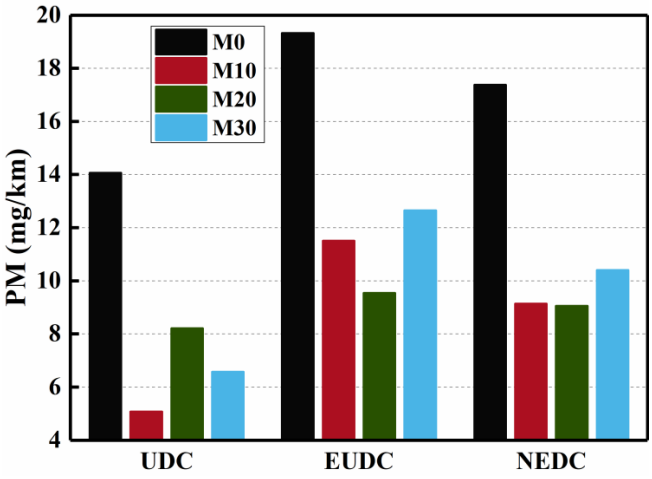

Figure 10. Effects of different methanol blending ratios on PM emissions under NEDC.

3.3. Effects of Blending Ratio of Methanol on Vehicle Acceleration

Figure 11 shows the effects of methanol blending ratio on vehicle acceleration. As the methanol blending ratio increases from 0 to 75%, the acceleration time of the vehicle shortens and the power performance enhances except for M50 and M75 at third gear, as seen from Figure 11. The variations of acceleration time of 3rd gear are not obvious, which may be related to the low speed of vehicle. The M50 and M75 with higher methanol blending ratio leads to lower in-cylinder temperature and insufficient combustion, resulting in slightly longer acceleration time of M50 and M75 than that of gasoline. At 4th gear, the acceleration time of M75 fuel is reduced by 0.9 s (11.7%) by comparison with that of M0. At 5th gear, the acceleration time of M75 fuel is reduced by 1.6 s (12.8%), relative to M0. This is mainly caused by the following three reasons. First of all, as mentioned above, methanol contains higher oxygen content than gasoline, which is beneficial to complete combustion and the improvement of power performance of the vehicle. Secondly, the relatively higher-octane number of methanol enhances the anti-knock performance, advances the spark timing automatically in the ECU, and increases the combustion constant volume degree; meanwhile, the relatively faster flame propagation speed of methanol shortens the combustion duration, which improves the power performance and shortens the acceleration time [64]. Finally, the higher volatility of methanol favors the acceleration response of the engine and improves the power performance of the vehicle.

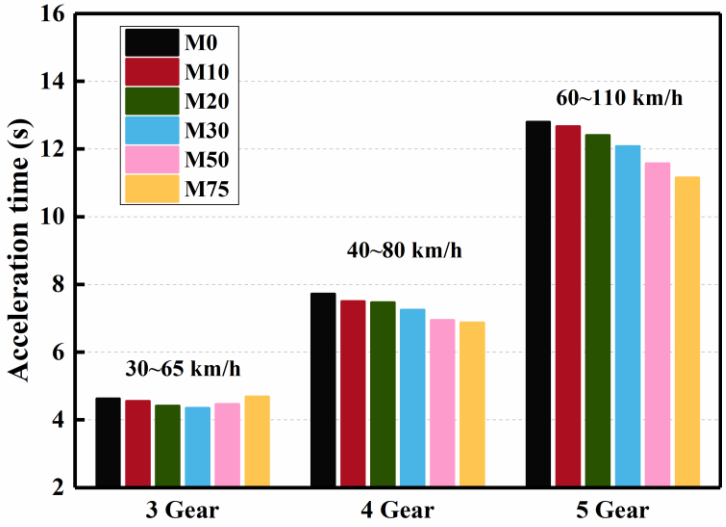

Figure 11. Effects of different methanol blending ratios on acceleration time at different gear speeds.

4. Conclusions

In the present study, a commercial GDI vehicle was applied to investigate the effects of five different volume blending ratios (10%, 20%, 30%, 50% and 75%) of methanol in methanol-gasoline blends on the fuel consumption and emissions characteristics in contrast with pure gasoline. The experiments were conducted on a chassis dynamometer, which can simulate the real driving conditions using the steady and NEDC approach. Furthermore, the power performance of the vehicle was analyzed in the acceleration test. The main conclusions are as follow:

(1) Under steady-state conditions, as the methanol blending ratio increases, the volume fuel consumption increases. Compared with M0, the equivalent fuel consumption of M75 is reduced by 0.95 L/100 km (10.6%) at 15 km/h. In terms of gaseous emissions, CO_2 emissions almost decrease in proportion with the blend ratio. The CO_2 emissions of M75 are reduced by 152.72 g/km (77.4%) at the speed of 15 km/h compared with M0. After blending methanol in gasoline, the reduction degree of NO_x emissions is highest at the speed of 15 km/h. The maximum relative difference of NO_x emissions is obtained by fueling M0 and M75, respectively, which differs by 79.1% (345.54 mg/km). CO emissions decrease after gasoline blended with methanol in most cases. Compared with M0, the CO emissions of M75 are reduced by 4491.4 mg/km (70.2%) at the speed of 15 km/h. With the increase in the methanol blending ratio, the THC emissions decrease asymptotically at medium and high vehicle speeds. The maximum relative difference of THC emissions is obtained by fueling M0 and M30 at 15 km/h, respectively, which differs by 59.9% (1225.48 mg/km).

(2) In the NEDC, as the blending ratio of methanol increases, the equivalent fuel consumption decreases. Compared with M0, the equivalent fuel consumption of M30 is reduced by 0.11 L/100 km (1.67%). Regarding gaseous emissions, the difference value between the minimum and maximum CO_2 emissions is 47.57 g/km (32.6%) by fueling M30 and M0 in the NEDC. NO_x emissions decrease with the increase of the blending ratio of methanol. The difference value between the minimum and maximum NO_x emissions is 194.66 mg/km (19.3%) by fueling M30 and M0, respectively. After blending methanol, CO emissions increase, and THC emissions decrease. Compared with M0, the emissions of CO and THC of M30 are increased by 1052.54 mg/km (24.1%) and decreased by 111.31 mg/km (10.9%), respectively. Concerning PM emissions, the difference between the minimum and maximum PM emissions is obtained by fueling M20 and M0, respectively, which differs by 8.32 mg/km (47.9%).

(3) With the blending ratio of methanol from 0% to 75%, the acceleration time of the vehicle shortens and the power performance enhances except for M75 at third gear. Compared to M0, the acceleration time of M75 is reduced by 0.9 s (11.7%) and 1.6 s (12.8%) at 4th and 5th gear, respectively.

The results demonstrated that as the blending ratio of methanol increases, the CO_2, NO_x, THC, and PM emissions, equivalent fuel consumption and acceleration time are reduced. However, since the requirement of cold start under NEDC, a higher methanol blend ratio to NEDC was not completed. Further investigations are required to increase the intake temperature by electric heater, increase the energy of spark ignition and using higher compression ratio, etc.

If the MAP in ECU is not calibrated again, the fuels are alternated directly. The vehicle cannot be cold start at the methanol blending ratios with more than 30%. In the NEDC, CO emissions increase, and the emissions of CO_2, NO_x, THC, and PM decrease fueled with methanol-gasoline blends with less than 30% methanol blending ratios. The acceleration time is shortened with the increase of blending ratio of methanol.

Author Contributions: Z.Z.: Methodology, Formal analysis, Writing-Original Draft. M.W.: Methodology, Software, Formal analysis. H.L.: Funding acquisition, Conceptualization, Investigation, Writing-Review & Editing. Y.C.: Software, Formal analysis, Writing-Review & Editing. Z.M.: Validation, Formal analysis. T.W.: Validation, Software. C.Z.: Validation, Writing-Review & Editing. J.D.A.:

Validation. C.J.: Validation. H.H.: Writing-Review & Editing. All authors have read and agreed to the published version of the manuscript.

Funding: The authors would like to acknowledge the financial support to the research provided by the National Natural Science Foundation of China through the Project of 52176125 and 51922076.

Institutional Review Board Statement: Not applicable.

Informed Consent Statement: Not applicable.

Data Availability Statement: All data used to support the findings of this study are included within the article.

Conflicts of Interest: The authors declare that they have no known competing financial interests that could have appeared to affect the work reported in this paper.

References

1. Salam, S.; Choudhary, T.; Pugazhendhi, A.; Verma, T.N.; Sharma, A. A review on recent progress in computational and empirical studies of compression ignition internal combustion engine. *Fuel* **2020**, *279*, 118469. [CrossRef]
2. Mahmudul, H.M.; Hagos, F.Y.; Mamat, R.; Adam, A.A.; Ishak, W.F.W.; Alenezi, R. Production, characterization and performance of biodiesel as an alternative fuel in diesel engines—A review. *Renew. Sustain. Energy Rev.* **2017**, *72*, 497–509. [CrossRef]
3. Yusri, I.; Mamat, R.; Najafi, G.; Razman, A.; Awad, O.; Azmi, W.; Ishak, I.D.M.S.A.; Shaiful, A. Alcohol based automotive fuels from first four alcohol family in compression and spark ignition engine: A review on engine performance and exhaust emissions. *Renew. Sustain. Energy Rev.* **2017**, *77*, 169–181. [CrossRef]
4. Rajak, U.; Verma, T.N. Spirulina microalgae biodiesel—A novel renewable alternative energy source for compression ignition engine. *J. Clean. Prod.* **2018**, *201*, 343–357. [CrossRef]
5. Yee, K.F.; Mohamed, A.R.; Tan, S.H. A review on the evolution of ethyl tert-butyl ether (ETBE) and its future prospects. *Renew. Sustain. Energy Rev.* **2013**, *22*, 604–620. [CrossRef]
6. Jin, C.; Zhang, X.; Han, W.; Geng, Z.; Thomas, M.T.M.; Jeffrey, A.D.; Wang, G.; Ji, J.; Liu, H. Macro and micro solubility between low-carbon alcohols and rapeseed oil using different co-solvents. *Fuel* **2020**, *270*, 117511. [CrossRef]
7. Zheng, Z.; Xia, M.; Liu, H.; Shang, R.; Ma, G.; Yao, M. Experimental study on combustion and emissions of n-butanol/biodiesel under both blended fuel mode and dual fuel RCCI mode. *Fuel* **2018**, *226*, 240–251. [CrossRef]
8. Liu, J.; Liu, Z.; Wang, L.; Wang, P.; Sun, P.; Ma, H.; Wu, P. Effects of PODE/diesel blends on particulate matter emission and particle oxidation characteristics of a common-rail diesel engine. *Fuel Process. Technol.* **2020**, *212*, 106634. [CrossRef]
9. Solouk, A.; Tripp, J.; Shakiba-Herfeh, M.; Shahbakhti, M. Fuel consumption assessment of a multi-mode low temperature combustion engine as range extender for an electric vehicle. *Energy Convers. Manag.* **2017**, *148*, 1478–1496. [CrossRef]
10. Hwang, J.-J.; Kuo, J.-K.; Wu, W.; Chang, W.-R.; Lin, C.-H.; Wang, S.-E. Lifecycle performance assessment of fuel cell/battery electric vehicles. *Int. J. Hydrogen Energy* **2013**, *38*, 3433–3446. [CrossRef]
11. Han, X.; Li, F.; Zhang, T.; Zhang, T.; Song, K. Economic energy management strategy design and simulation for a dual-stack fuel cell electric vehicle. *Int. J. Hydrogen Energy* **2017**, *42*, 11584–11595. [CrossRef]
12. Ma, H.; Balthasar, F.; Tait, N.; Riera-Palou, X.; Harrison, A. A new comparison between the life cycle greenhouse gas emissions of battery electric vehicles and internal combustion vehicles. *Energy Policy* **2012**, *44*, 160–173. [CrossRef]
13. Wachtmeister, H.; Henke, P.; Höök, M. Oil projections in retrospect: Revisions, accuracy and current uncertainty. *Appl. Energy* **2018**, *220*, 138–153. [CrossRef]
14. Zhen, X.; Wang, Y.; Xu, S.; Zhu, Y. Numerical analysis on knock for a high compression ratio spark-ignition methanol engine. *Fuel* **2013**, *103*, 892–898. [CrossRef]
15. Kalghatgi, G. Is it really the end of internal combustion engines and petroleum in transport? *Appl. Energy* **2018**, *225*, 965–974. [CrossRef]
16. Melton, N.; Axsen, J.; Sperling, D. Moving beyond alternative fuel hype to decarbonize transportation. *Nat. Energy* **2016**, *1*, 16013. [CrossRef]
17. Hwang, J.G.; Choi, M.K.; Choi, D.H.; Choi, H.S. Quality improvement and tar reduction of syngas produced by bio-oil gasification. *Energy* **2021**, *236*, 121473. [CrossRef]
18. Rakopoulos, D.C.; Rakopoulos, C.; Giakoumis, E.G.; Komninos, N.P.; Kosmadakis, G.M.; Papagiannakis, R.G. Comparative Evaluation of Ethanol, n-Butanol, and Diethyl Ether Effects as Biofuel Supplements on Combustion Characteristics, Cyclic Variations, and Emissions Balance in Light-Duty Diesel Engine. *J. Energy Eng.* **2017**, *143*, 04016044. [CrossRef]
19. Shenbagamuthuraman, V.; Patel, A.; Khanna, S.; Banerjee, E.; Parekh, S.; Karthick, C.; Ashok, B.; Velvizhi, G.; Nanthagopal, K.; Ong, H.C. State of art of valorising of diverse potential feedstocks for the production of alcohols and ethers: Current changes and perspectives. *Chemosphere* **2021**, *286*, 131587. [CrossRef]
20. Saiteja, P.; Ashok, B. A critical insight review on homogeneous charge compression ignition engine characteristics powered by biofuels. *Fuel* **2020**, *285*, 119202. [CrossRef]

21. Kumar, T.S.; Ashok, B. Critical review on combustion phenomena of low carbon alcohols in SI engine with its challenges and future directions. *Renew. Sustain. Energy Rev.* **2021**, *152*, 111702. [CrossRef]
22. Karthick, C.; Nanthagopal, K.; Ashok, B.; Saravanan, S.V. Influence of alcohol and gaseous fuels on NOx reduction in IC engines. In *NOx Emission Control Technologies in Stationary and Automotive Internal Combustion Engines*; Elsevier: Amsterdam, The Netherlands, 2022; pp. 347–385. [CrossRef]
23. Wen, M.; Zhang, C.; Yue, Z.; Liu, X.; Yang, Y.; Dong, F.; Liu, H.; Yao, M. Effects of Gasoline Octane Number on Fuel Consumption and Emissions in Two Vehicles Equipped with GDI and PFI Spark-Ignition Engine. *J. Energy Eng.* **2020**, *146*, 04020069. [CrossRef]
24. Sankesh, D.; Lappas, P. An experimental and numerical study of natural gas jets for direct injection internal combustion engines. *Fuel* **2019**, *263*, 116745. [CrossRef]
25. Amador, G.; Yepes, H.A.; Gonzalez-Quiroga, A.; Bula, A. Development of extended formulations of the relative concentration of chain carrier method for knock prediction in spark-ignited internal combustion engines fueled with gaseous fuels. *Fuel* **2020**, *279*, 118352. [CrossRef]
26. Pickl, F.; Russer, M.; Hauenstein, M.; Wensing, M. Modelling and understanding deposit formation and reduction in combustion engines—Application to the concrete case of internal GDI injector deposit. *Fuel* **2018**, *236*, 284–296. [CrossRef]
27. Diaz, G.J.A.; Martinez, L.M.C.; Montoya, J.P.G.; Olsen, D.B. Methane number measurements of hydrogen/carbon monoxide mixtures diluted with carbon dioxide for syngas spark ignited internal combustion engine applications. *Fuel* **2018**, *236*, 535–543. [CrossRef]
28. Rakopoulos, D.C.; Rakopoulos, C.; Papagiannakis, R.G.; Giakoumis, E.G.; Karellas, S.; Kosmadakis, G.M. Combustion and Emissions in an HSDI Engine Running on Diesel or Vegetable Oil Base Fuel with n-Butanol or Diethyl Ether As a Fuel Extender. *J. Energy Eng.* **2016**, *142*, E4015006. [CrossRef]
29. Chen, Z.; Zhang, Y.; Wei, X.; Zhang, Q.; Wu, Z.; Liu, J. Thermodynamic process and performance of high n-butanol/gasoline blends fired in a GDI production engine running wide-open throttle (WOT). *Energy Convers. Manag.* **2017**, *152*, 57–64. [CrossRef]
30. Chen, Z.; Yang, F.; Xue, S.; Wu, Z.; Liu, J. Impact of higher n-butanol addition on combustion and performance of GDI engine in stoichiometric combustion. *Energy Convers. Manag.* **2015**, *106*, 385–392. [CrossRef]
31. Li, J.; Gong, C.-M.; Su, Y.; Dou, H.-L.; Liu, X.-J. Effect of injection and ignition timings on performance and emissions from a spark-ignition engine fueled with methanol. *Fuel* **2010**, *89*, 3919–3925. [CrossRef]
32. Qian, Y.; Liu, G.; Guo, J.; Zhang, Y.; Zhu, L.; Lu, X. Engine performance and octane on demand studies of a dual fuel spark ignition engine with ethanol/gasoline surrogates as fuel. *Energy Convers. Manag.* **2019**, *183*, 296–306. [CrossRef]
33. Al-Farayedhi, A.A.; Al-Dawood, A.M.; Gandhidasan, P. Experimental Investigation of SI Engine Performance Using Oxygenated Fuel. *J. Eng. Gas Turbines Power* **2004**, *126*, 178–191. [CrossRef]
34. Verhelst, S.; Turner, J.W.; Sileghem, L.; Vancoillie, J. Methanol as a fuel for internal combustion engines. *Prog. Energy Combust. Sci.* **2018**, *70*, 43–88. [CrossRef]
35. Yang, C.-J.; Jackson, R.B. China's growing methanol economy and its implications for energy and the environment. *Energy Policy* **2012**, *41*, 878–884. [CrossRef]
36. Dai, P.; Ge, Y.; Lin, Y.; Su, S.; Liang, B. Investigation on characteristics of exhaust and evaporative emissions from passenger cars fueled with gasoline/methanol blends. *Fuel* **2013**, *113*, 10–16. [CrossRef]
37. Jin, C.; Zhang, X.; Geng, Z.; Pang, X.; Wang, X.; Ji, J.; Wang, G.; Liu, H. Effects of various co-solvents on the solubility between blends of soybean oil with either methanol or ethanol. *Fuel* **2019**, *244*, 461–471. [CrossRef]
38. Thiyagarajan, S.; Sonthalia, A.; Geo, V.E.; Prakash, T.; Karthickeyan, V.; Ashok, B.; Nanthagopal, K.; Dhinesh, B. Effect of manifold injection of methanol/n-pentanol in safflower biodiesel fuelled CI engine. *Fuel* **2019**, *261*, 116378. [CrossRef]
39. Smith, J.K.; Roberts, P.; Kountouriotis, A.; Richardson, D.; Aleiferis, P.; Ruprecht, D. Thermodynamic modelling of a stratified charge spark ignition engine. *Int. J. Engine Res.* **2018**, *21*, 801–810. [CrossRef]
40. Chen, T.; Wang, X.; Zhao, H.; Xie, H.; He, B. Control and optimization of spark ignition–controlled auto-ignition hybrid combustion based on stratified flame ignition. *Proc. Inst. Mech. Eng. Part D J. Automob. Eng.* **2018**, *233*, 3057–3073. [CrossRef]
41. He, X.; Zhou, Y.; Liu, Z.; Yang, Q.; Sjöberg, M.; Vuilleumier, D.; Ding, C.-P.; Liu, F. Impact of coolant temperature on the combustion characteristics and emissions of a stratified-charge direct-injection spark-ignition engine fueled with E30. *Fuel* **2021**, *309*, 121913. [CrossRef]
42. Chen, H.; Yang, L.; Zhang, P.-H.; Harrison, A. The controversial fuel methanol strategy in China and its evaluation. *Energy Strat. Rev.* **2014**, *4*, 28–33. [CrossRef]
43. Szybist, J.P.; Splitter, D. Pressure and temperature effects on fuels with varying octane sensitivity at high load in SI engines. *Combust. Flame* **2017**, *177*, 49–66. [CrossRef]
44. Wang, B.; Yao, A.; Chen, C.; Yao, C.; Wang, H.; Liu, M.; Li, Z. Strategy of improving fuel consumption and reducing emission at low load in a diesel methanol dual fuel engine. *Fuel* **2019**, *254*, 115660. [CrossRef]
45. Li, X.; Zhen, X.; Wang, Y.; Liu, D.; Tian, Z. The knock study of high compression ratio SI engine fueled with methanol in combination with different EGR rates. *Fuel* **2019**, *257*, 116098. [CrossRef]
46. Shamun, S.; Haşimoğlu, C.; Murcak, A.; Andersson, Ö.; Tunér, M.; Tunestål, P. Experimental investigation of methanol compression ignition in a high compression ratio HD engine using a Box-Behnken design. *Fuel* **2017**, *209*, 624–633. [CrossRef]

47. Lvarez, A.; Bansode, A.; Urakawa, A.; Bavykina, A.V.; Wezendonk, T.A.; Makkee, M.; Gascon, J.; Kapteijn, F. Challenges in the Greener Production of Formates/Formic Acid, Methanol, and DME by Heterogeneously Catalyzed CO_2 Hydrogenation Processes. *Chem. Rev.* **2017**, *117*, 9804–9838. [CrossRef]
48. Chen, W.-H.; Lin, B.-J.; Lee, H.-M.; Huang, M.-H. One-step synthesis of dimethyl ether from the gas mixture containing CO_2 with high space velocity. *Appl. Energy* **2012**, *98*, 92–101. [CrossRef]
49. Halder, A.; Kilianová, M.; Yang, B.; Tyo, E.C.; Seifert, S.; Prucek, R.; Panáček, A.; Suchomel, P.; Tomanec, O.; Gosztola, D.J.; et al. Highly efficient Cu-decorated iron oxide nanocatalyst for low pressure CO_2 conversion. *Appl. Catal. B Environ.* **2018**, *225*, 128–138. [CrossRef]
50. Lian, H.-Y.; Li, X.-S.; Liu, J.-L.; Zhu, A.-M. Methanol steam reforming by heat-insulated warm plasma catalysis for efficient hydrogen production. *Catal. Today* **2019**, *337*, 76–82. [CrossRef]
51. Bansode, A.; Urakawa, A. Towards full one-pass conversion of carbon dioxide to methanol and methanol-derived products. *J. Catal.* **2014**, *309*, 66–70. [CrossRef]
52. Liu, S.; Clemente, E.R.C.; Hu, T.; Wei, Y. Study of spark ignition engine fueled with methanol/gasoline fuel blends. *Appl. Therm. Eng.* **2007**, *27*, 1904–1910. [CrossRef]
53. Nuthan Prasad, B.S.; Pandey, J.K.; Kumar, G.N. Impact of changing compression ratio on engine characteristics of an SI engine fueled with equi-volume blend of methanol and gasoline. *Energy* **2020**, *191*, 116605. [CrossRef]
54. Maurya, R.K.; Agarwal, A. Experimental investigations of performance, combustion and emission characteristics of ethanol and methanol fueled HCCI engine. *Fuel Process. Technol.* **2014**, *126*, 30–48. [CrossRef]
55. Hua, Y.; Liu, F.; Wu, H.; Kang, N.; Shi, Z. *Soot and PAH Formation Characteristics of Methanol-Gasoline Belnds in Laminar Coflow Diffusion Flames*; SAE International: Warrendale, PA, USA, 2018. [CrossRef]
56. Wei, Y.; Liu, S.; Liu, F.; Liu, J.; Zhu, Z.; Li, G. Formaldehyde and Methanol Emissions from a Methanol/Gasoline-Fueled Spark-Ignition (SI) Engine. *Energy Fuels* **2009**, *23*, 3313–3318. [CrossRef]
57. Zhang, F.; Zhang, X.; Shuai, S.; Xiao, J.; Wang, J. Unregulated Emissions and Combustion Characteristics of Low-Content Methanol−Gasoline Blended Fuels. *Energy Fuels* **2010**, *24*, 1283–1292. [CrossRef]
58. Li, J.; Gong, C.; Liu, B.; Su, Y.; Dou, H.; Liu, X. Combustion and Hydrocarbon (HC) Emissions from a Spark-Ignition Engine Fueled with Gasoline and Methanol during Cold Start. *Energy Fuels* **2009**, *23*, 4937–4942. [CrossRef]
59. Wang, X.; Ge, Y.; Liu, L.; Peng, Z.; Hao, L.; Yin, H.; Ding, Y.; Wang, J. Evaluation on toxic reduction and fuel economy of a gasoline direct injection- (GDI-) powered passenger car fueled with methanol–gasoline blends with various substitution ratios. *Appl. Energy* **2015**, *157*, 134–143. [CrossRef]
60. Liu, H.; Wang, X.; Zhang, D.; Dong, F.; Liu, X.; Yang, Y.; Huang, H.; Wang, Y.; Wang, Q.; Zheng, Z. Investigation on Blending Effects of Gasoline Fuel with N-Butanol, DMF, and Ethanol on the Fuel Consumption and Harmful Emissions in a GDI Vehicle. *Energies* **2019**, *12*, 1845. [CrossRef]
61. Liu, H.; Zhang, C.; Wen, M.; Zhang, D.; Yang, Y.; Liu, X. Experimental study on vehicle performance and emissions of different oxygenated gasoline fuels. *Chin. Intern. Combust. Engine Eng.* **2019**, *40*, 8. [CrossRef]
62. Kalwar, A.; Singh, A.P.; Agarwal, A.K. Utilization of primary alcohols in dual-fuel injection mode in a gasoline direct injection engine. *Fuel* **2020**, *276*, 118068. [CrossRef]
63. Liu, H.; Yao, M.; Zhang, B.; Zheng, Z. Effects of Inlet Pressure and Octane Numbers on Combustion and Emissions of a Homogeneous Charge Compression Ignition (HCCI) Engine. *Energy Fuels* **2008**, *22*, 2207–2215. [CrossRef]
64. Nguyen, D.-K.; Sileghem, L.; Verhelst, S. A quasi-dimensional combustion model for spark ignition engines fueled with gasoline–methanol blends. *Proc. Inst. Mech. Eng. Part D J. Automob. Eng.* **2017**, *232*, 57–74. [CrossRef]